Penton Release from P22 Heat-Expanded Capsids Suggests Importance of Stabilizing Penton-Hexon Interactions during Capsid Maturation

Carolyn M. Teschke,* Amy McGough,† and Pamela A. Thuman-Commike‡
*Department of Molecular and Cell Biology, University of Connecticut, Storrs, Connecticut 06269; †Department of Biological Sciences and Markey Center for Structural Biology, Purdue University, West Lafayette, Indiana 47907; and ‡QED Labs, San Jose, California 95128

ABSTRACT Bacteriophage assembly frequently begins with the formation of a precursor capsid that serves as a DNA packaging machine. The DNA packaging is accompanied by a morphogenesis of the small round precursor capsid into a large polyhedral DNA-containing mature phage. In vitro, this transformation can be induced by heat or chemical treatment of P22 procapsids. In this work, we examine bacteriophage P22 morphogenesis by comparing three-dimensional structures of capsids expanded both in vitro by heat treatment and in vivo by DNA packaging. The heat-expanded capsid reveals a structure that is virtually the same as the in vivo expanded capsid except that the pentons, normally present at the icosahedral fivefold positions, have been released. The similarities of these two capsid structures suggest that the mechanism of heat expansion is similar to in vivo expansion. The loss of the pentons further suggests the necessity of specific penton-hexon interactions during expansion. We propose a model whereby the penton-hexon interactions are stabilized through interactions of DNA, coat protein, and other minor proteins. When considered in the context of other studies using chemical or heat treatment of capsids, our study indicates that penton release may be a common trend among double-stranded DNA containing viruses.

INTRODUCTION

Viruses such as the herpesviruses (Rixon, 1993) and adenoviruses (D'Halluin et al., 1978) and some bacteriophage including lambda, HK97, T4, and P22 actively package double-stranded DNA (dsDNA) into preformed precursor capsids known as procapsids (Casjens and Hendrix, 1988; King and Chiu, 1997). During packaging of the viral or phage genomes, these procapsids undergo complex structural transitions in a process called maturation. Characteristic features of maturation are the removal of internal scaffolding protein accompanied by conformational changes of the capsid protein resulting in capsid lattice rearrangements and enlargement of overall capsid capacity. These structural rearrangements stabilize the capsid thereby protecting the genome residing within the virus.

In the *Salmonella* bacteriophage P22, 420 molecules of folded monomeric coat protein interact with 150–300 molecules of scaffolding protein, a portal protein complex, and pilot proteins to form the procapsid (King et al., 1976; King and Chiu, 1997). DsDNA is actively packaged into the P22 procapsid by DNA packaging proteins accompanied by scaffolding protein exit through holes in the procapsid lattice (Bazinet and King, 1985; King and Casjens, 1974; King et al., 1973). A structural transformation from the procapsid lattice to the mature virus also occurs during DNA packaging, increasing the average diameter of the capsid by 10% (Zhang et al., 2000). Within the resulting mature phage, the DNA is tightly packed within the capsid to the density of liquid crystal (Cerritelli et al., 1997; Lepault et al., 1987), so the capsid must also be stable enough to counter the force of such a highly packed ionic material.

Distinct energies and forces are used in the assembly and maturation processes. Assembly of P22 procapsids proceeds through specific protein:protein interactions without the input of an additional energy source such as ATP. Interactions between coat proteins seem to be primarily hydrophobic (Teschke and King, 1993) whereas coat protein-scaffolding protein interactions are ionic in nature (Parker and Prevelige, 1998). In contrast, a precursor capsid will not undergo the structural transition to the mature viral capsid without some energy input (Galisteo and King, 1993; Tuma et al., 1998). In vivo, this energy is derived from the DNA packaging ATPases (Botstein et al., 1973; King et al., 1978). In vitro, physical forces such as the addition of heat or low concentrations of agents that destabilize protein structure, such as sodium dodecyl sulfate (SDS) or denaturants, will induce the expansion of precursor capsids to the mature viral lattice (Capen and Teschke, 2000; Earnshaw et al., 1976; Galisteo and King, 1993). Since the capsids do not dissociate during expansion, the forces involved in expansion must not be greater than those involved in the protein:protein interactions that hold the capsid together or be compensated for by additional interactions such as capsid protein:DNA interactions. Indeed, expansion in P22 produces 90 kJ/mol of exothermic energy, only around 5% of the energy required for capsid denaturation (Galisteo and King, 1993; Steven, 1993).

In previous investigations of bacteriophage P22 morphogenesis, heat has been the most frequently used method to induce the structural transition from the procapsid to the expanded viral lattice in vitro. The presumption in these studies was that the heat-induced expanded structure was identical to the in vivo-expanded structure as judged by low-resolution negative-stain electron micrographs of both structures (Galisteo and King, 1993). Here, we have determined the

Submitted May 26, 2002, and accepted for publication December 12, 2002.

Address reprint requests to Pamela A. Thuman-Commike, Tel.: 408-295-8347; Fax: 408-295-8348; E-mail: pam@qedlabs.com.

0006-3495/03/04/2585/08 $2.00

structure of heat-expanded and in vivo-expanded P22 capsids by electron cryomicroscopy and three-dimensional reconstruction to determine whether the in vivo and in vitro expansion processes follow the same mechanism and result in the same capsid structure. Although we find that the dimensions of both structures are identical, the heat-expanded capsids have released coat protein subunits from the penton positions in the lattice. Our results lead us to suggest a model whereby the DNA and pilot proteins may play an additional important role in stabilizing penton-hexon interactions, as both are missing from the in vitro-expanded capsids, especially during the lattice transformation in maturation.

MATERIAL AND METHODS

Capsid preparation

Procapsids and in vivo-expanded empty phage heads were prepared as previously described (Galisteo and King, 1993; Prevelige et al., 1988; Teschke and Fong, 1996). Briefly, *Salmonella typhimurium* were grown at 28°C to 4×10^8 cells/mL and infected with either bacteriophage P22 carrying amber mutations in gene 2 or 3 so that DNA packaging is blocked resulting in production of procapsids, or an amber mutation in gene 4 that allows DNA packaging but does not maintain the DNA within the capsid resulting in in vivo-expanded heads that do not contain DNA. In both cases, an amber mutation in gene 13 that blocks cell lysis, was also used. The infected cells were grown for 4.5 h and pelleted by centrifugation. After suspension in a small amount of buffer, the cells were lysed by one or two freeze/thaw cycles. The thawed lysate was brought to a final concentration of 0.1 M phenylmethylsulfonyl fluoride (PMSF), treated with RNase and DNase, and the procapsids (from a 2- 13- amber or 3- 13- amber infection) or empty phage heads (from a 4- 13- amber infection) were pelleted in a Beckman L7-65 with a Ti60 rotor at 45,000 rpm for 35 min. The pellets of procapsids or empty phage heads were shaken overnight at 4°C in a small amount of buffer with PMSF and purified over a Sephacryl S1000 column (Pharmacia LKB, Uppsala, Sweden). The procapsids or empty phage heads were pelleted, suspended in buffer, and stored at 4°C.

Empty procapsid shells were prepared from procapsids by repeated treatment at 4°C with buffer containing PMSF and 0.5 M guanidine hydrochloride (GuHCl), which extracts scaffolding protein while leaving the empty capsid shells intact. After each incubation with GuHCl, the shells were pelleted as above and the pellets suspended in buffer. After the third extraction, the empty procapsid shells were stored in buffer at 4°C.

Heat-expanded capsids were obtained from procapsids or empty procapsid shells (1 mg/ml) that were incubated at 70°C for 15 min. This temperature and time were shown previously to cause >95% expansion of wild-type empty procapsid shells without loss of sample to aggregate (Capen and Teschke, 2000). To confirm that expansion had occurred, the samples were run on 1.2% Seakem HGT agarose gels (Capen and Teschke, 2000; Galisteo and King, 1993).

Electron cryomicroscopy and image processing

Capsid samples were applied to 400-mesh copper grids prepared with holey carbon films, rapidly plunged into liquid ethane, and imaged while maintained at −180°C using an FEI (Hillsboro, OR) CM200-FEG transmission electron microscope outfitted with a Gatan (Pleasanton, CA) cold holder, TV, and 1k × 1k CCD camera. Images were recorded using low dose conditions (10–12 $e^-/Å^2$) at an accelerating voltage of 200 kV and a nominal magnification of 38,000×. Electron micrographs were visually inspected for quality and particle distribution. Suitable micrographs were scanned using a Phodis/SCAI flatbed scanner (Z/I Imaging, Englewood, CO) with a step size of 7 μm, and then twofold averaged to an effective scan size of 3.68 Å per pixel.

Structure determination of capsids was performed similarly to previously determined bacteriophage P22 structures (Thuman-Commike et al., 1999). The heat-expanded capsid three-dimensional structure was determined using 134 particles imaged at ~1.7 μm underfocus and the in vivo-expanded empty phage head three-dimensional structure was determined using 105 particles imaged at ~2.0 μm underfocus. All particles were visually inspected to ensure no procapsid particles were selected or processed with the expanded particles. The final resolution of each reconstruction was verified to be 24 Å using the Fourier ring correlation coefficient (Radermacher, 1988; van Heel, 1987) and the amplitude-weighted mean phase difference (Frank et al., 1981). The difference maps were computed as the algebraic difference between all corresponding points in the reconstructions for which the density was at or above the contour threshold level (Marvik et al., 1995).

RESULTS

In vitro heat-expanded and in vivo-expanded capsids

Heat-expanded capsids were produced both with and without GuHCl treatment to release the scaffolding protein before heat expansion. In Fig. 1 *A*, each of the investigated samples was analyzed by SDS-PAGE. Both heat expansion and GuHCl treatment cause release of scaffolding protein from within the procapsid (Fuller and King, 1981; Galisteo and King, 1993). Empty phage heads were produced in vivo by allowing procapsids within infected cells to package DNA, but not to maintain the DNA within the phage capsids. During in vivo packaging, the scaffolding protein is released from the procapsid for use in further rounds of assembly and the capsid lattice expands (King and Casjens, 1974). Notice that the lane of in vivo-expanded empty phage heads in Fig. 1 *A* appears to have residual scaffolding protein. This is due to the presence of a small quantity of procapsids in the preparation.

In vivo-expanded empty phage heads were chosen for this investigation rather than phage heads that contain DNA because they allow us to more readily compare the features of the in vivo- and in vitro-expanded capsids without interference from the internal DNA. Fig. 1 *B* shows the migration of procapsids, heat-expanded capsids, and empty phage heads (i.e., in vivo-expanded capsids) on an agarose gel. In these gels, proteins migrate according to their surface charge:mass ratio. So at a constant charge, a decrease in mass of the proteins will cause the proteins to migrate further into the gel (Serwer et al., 1986). Empty procapsid shells that were treated with GuHCl run in the same position as procapsids (data not shown). The heat-expanded capsids run slower than procapsids on the agarose gel, as has been observed previously (Capen and Teschke, 2000; Galisteo and King, 1993). Notice also that the in vivo-expanded empty phage heads migrate further into the gel than the heat-expanded procapsids. As we find that the overall mass of the heat-expanded capsids is reduced (see below), the migration of the heat-expanded capsids must be different than the in vivo-expanded capsids because of either a change in diameter or surface charge, or both (Serwer et al., 1986). Both types of capsids have the same diameter (see below); consequently the

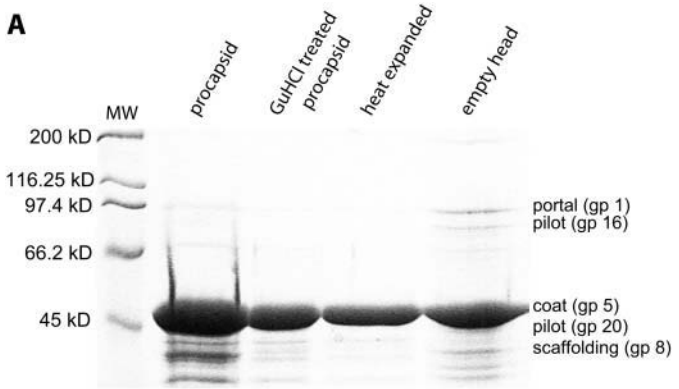

FIGURE 1 Comparison of procapsids, heat-expanded capsids, and in vivo-expanded capsids on (*A*) a 10% SDS-PAGE to evaluate protein composition and (*B*) a nondenaturing 1.2% agarose gel showing the change in expansion that occurs upon heat treatment. In panel *A*, the molecular weight markers are shown indicated on the right and the identity of the phage proteins on the left. In panel *B*, the poles for the electrophoresis are shown on the right.

change in migration must be due to an increase in overall charge to more basic.

Electron cryomicroscopy and image processing

Image reconstruction was performed on both the in vitro- and in vivo-expanded capsids with each showing comparable results during all stages of data processing and in the resulting three-dimensional reconstructions. For simplicity, in the following we show the data associated with the heat-expanded capsid that was not treated with GuHCl before heat treatment. Fig. 2, *A* and *B*, show the resulting electron cryomicroscopy images. Notice that overall the heat-expanded capsid appears as a spherical thin-shelled empty capsid (Fig. 2 *A*) whereas the in vivo-expanded empty phage head appears as a larger polyhedral capsid (Fig. 2 *B*).

The three-dimensional heat-expanded capsid structure reveals that the capsid is a $T = 7$ icosahedron that lacks the five subunits positioned around the icosahedral fivefold axis (Fig. 3). The absence of these five subunits results in the spherical appearance of the heat-expanded capsids in the images (Fig. 2 *A*). It should be noted, however, that the heat-expanded capsid is actually polyhedral in that the unit triangle with vertices at the fivefold axis is primarily flat in contrast to the curved unit triangle that is present in the spherical precursor procapsid (Prasad et al., 1993). Thus, the heat-expanded capsids appear spherical because the pentons of coat protein positioned at the icosahedral fivefold positions have been released from the capsid (Fig. 3 *A*) during heat expansion. The heat-expanded structure is consistent with the results of our nondenaturing agarose gel; the change in mobility of the heat-expanded capsids is likely the result of the release of the pentons, thereby exposing basic subunit interfaces. In support of our observation, the surfaces between neighboring subunits of the distantly related phage HK97 have been shown to have many basic amino acids (Conway et al., 2001).

Comparison of heat-expanded capsid to in vivo-expanded empty phage head

Visual comparison of the heat-expanded capsid (Fig. 3 *A*) to the in vivo-expanded empty phage head (Fig. 3 *B*)

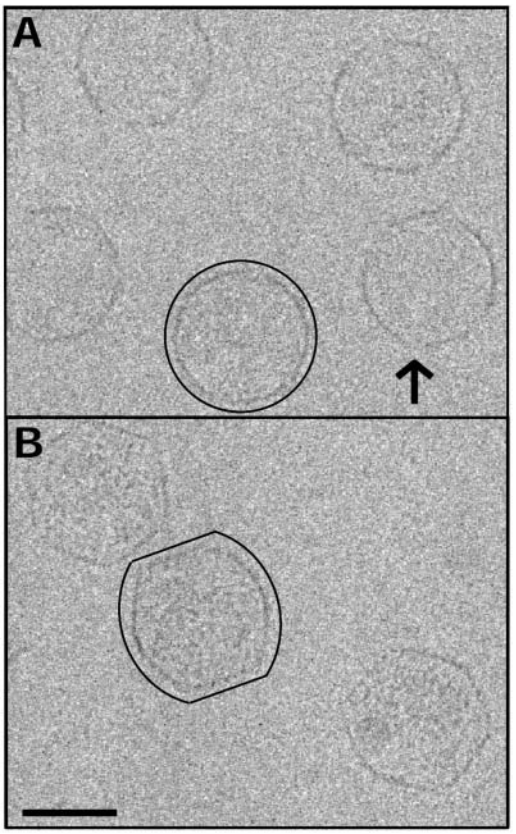

FIGURE 2 Selected regions of 200kv FEG electron cryomicroscopy images of (*A*) heat-expanded capsids and (*B*) in vivo-expanded empty phage heads. The arrow indicates an apparent hole in the shell of the heat-expanded capsid. The outlines around two of the capsids demonstrate the more spherical shape of the heat-expanded capsid compared to the in vivo-expanded empty head. Scale bar, 500 Å.

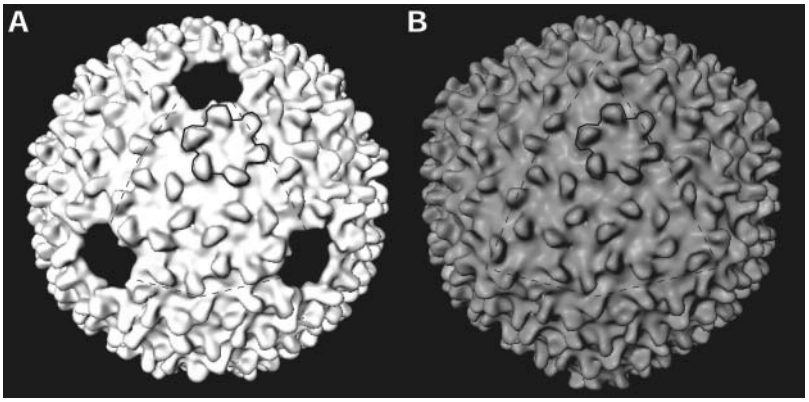

FIGURE 3 Outer surface representation of (*A*) the heat-expanded capsid and (*B*) the in vivo-expanded empty head three-dimensional reconstructions viewed from the icosahedral threefold axis. The unit triangle and one hexon have been outlined on each capsid for a point of reference.

shows that the capsids are remarkably similar. Both have skewed hexons and flat faces. The heat-expanded capsid has a maximal outer diameter of 680 Å and an average outer diameter of 585 Å. The in vivo-expanded empty phage head has a maximal outer diameter of 710 Å and an average outer diameter of 585 Å. Although the diameter of the empty phage head appears significantly larger, this additional size is a result of the protruding pentons present in the in vivo-expanded empty phage head. The shells of both capsids are ~45 Å thick and extend to an inner radius of 270 Å.

Quantitative comparison using difference maps confirms the capsids are very similar (Fig. 4, *A–D*). The most significant differences, visible to beyond 3 σ above the mean in the difference maps, appear at the regions surrounding the penton positions on the outer surface of the heat-expanded capsid (Fig. 4 *A*) and on the inner surface of the in vivo-expanded empty head (Fig. 4 *D*). These differences result from the absence of the pentons in the heat-expanded capsid (Fig. 4 *A*, *outlined region*) and from the coat proteins located nearest to the penton hole, on the heat-expanded capsid, residing at a lower radius than those of the in vivo-expanded empty phage head (Fig. 4 *D*, *outlined region*). In addition, smaller, less significant differences, visible to only 2 σ above the mean in the difference maps, appear just beneath the inner surface of the in vivo-expanded empty phage head (data not shown). These differences are near the proposed regions of coat/scaffold interaction (Thuman-Commike et al., 1999). No significant differences are observed on the outer in vivo-expanded empty head or inner heat-expanded capsid (Fig. 4, *B* and *C*).

Variability of released pentons

Examination of the fivefold region of the heat-expanded capsids at different density levels shows some variability in the absence of the coat subunits at the penton position (Fig. 5, *A–D*). Specifically, at a density level corresponding to 1.0 σ above the mean (Fig. 5 *C*), a small amount of density is observed at the penton, and at 0.75 σ above the mean (Fig. 5 *D*), a partial penton is observed.

To examine the nature of this variability, we performed a computational comparison of three-dimensional structures generated from various ratios of computed projection images using the heat-expanded capsid and in vivo-expanded empty phage head reconstructions. In this comparison we examined the simulated reconstruction of a capsid composed of x percent of the in vivo-expanded empty phage head computed projection images and y percent of heat-expanded capsid images to identify a ratio that produced similar visible penton density to that of the heat-expanded capsid structure. We found that using 2–4% in vivo-expanded empty phage head images combined with 98–96% heat-expanded capsid images, the density located at the penton position is observable at the same σ-levels as in the heat expanded capsid reconstruction. Since our three-dimensional reconstruction of the heat expanded capsid consists of ~150 images, this means that one of the following is a possible configuration of the heat-expanded capsids in our reconstruction: 4–6 capsids have not lost any pentons, one penton within every three capsids has not been released, or two pentons in every six capsids have not been released, etc. Although we cannot predict the particular mixture of nonreleased pentons, these results demonstrate that the total number of non-released penton is small and not likely to be of significant consequence.

DISCUSSION

Heat expansion is comparable to in vivo expansion

Our results show that in vitro-expanded capsids are the same as in vivo-expanded capsids except that the pentons have been released. Heat-expanded capsids are routinely used in experiments in place of in vivo-expanded capsids (Capen and Teschke, 2000; Galisteo and King, 1993; Parker and Prevelige, 1998; Teschke and Fong, 1996; Tuma et al., 1998). The overall similarities of the heat-expanded capsids validate

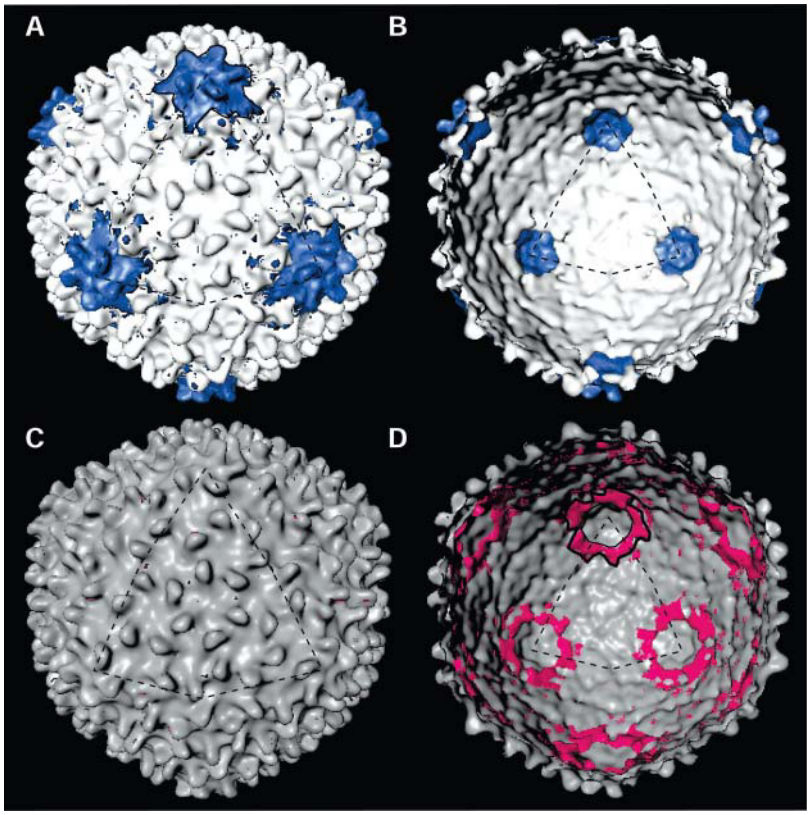

FIGURE 4 Difference maps denoting the significant differences between the heat-expanded and in vivo-expanded empty head capsids. Algebraic difference maps (Marvik et al., 1995) were used to identify and confirm statistically significant structural differences. The densities are displayed at 2 σ above the mean of the difference map. (*A–B*) In white is the surface representation of the heat-expanded capsid and shown in blue is the difference map representing features present in the empty phage head but absent from the heat-expanded capsid. (*C–D*) In gray is the surface representation of the in vivo-expanded empty phage head and shown in pink is the difference map representing features present in the heat-expanded capsid but absent from the empty phage head. The left panels are a view of the outer surface and the right panels are a view of the inner surface. The outlined regions denote the differences significant to beyond 3 σ above the mean of the difference maps and are attributable to the loss of the pentons. The position of the unit triangle is outlined on both the inner and outer surface as a point of reference.

many of these previous studies using heat-expanded capsids. The caveat is that our results also demonstrate that heat-expanded capsids lack pentons. Thus, heat-expanded capsids have large (100 Å diameter) holes not present in the in vivo-expanded capsids. We should note that our observations do not indicate if the heat expansion follows the same pathway as in vivo expansion except that the resulting structure is the same apart from the loss of pentons.

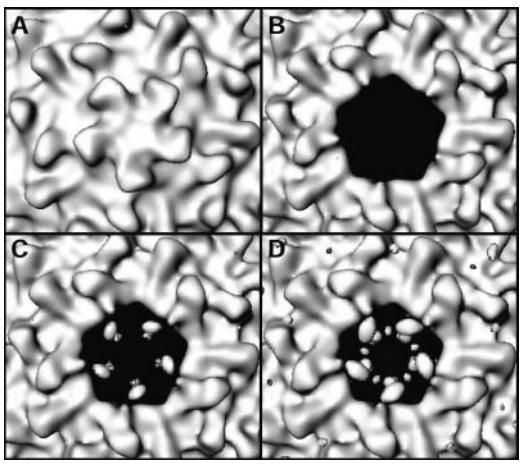

FIGURE 5 Zoomed-in view of the penton position for the (*A*) in vivo-expanded empty head and (*B–D*) heat-expanded capsid. The empty head in panel *A* and the heat-expanded capsid in panel *B* are shown at a density level of 1.5 σ above the mean. The heat-expanded capsid in panel *C* is shown at 1.0 σ above the mean and in panel *D* it is shown at 0.75 σ above the mean. Notice that as the contour threshold decreases, additional density becomes visible at the heat-expanded penton. Thresholds beyond 0.75 σ above the mean contain large amounts of noise, indicating any additional density displayed for the penton is not statistically significant.

In vitro heat expansion affects penton-hexon interactions

The absence of pentons in heat-expanded capsids suggests a destabilization of the coat protein:coat protein interactions between neighboring penton and hexon subunits that results in the release of the pentons. Our observations do not indicate if this release takes place during or after expansion has occurred. To answer this question, we heated both in vivo-expanded capsids with and without DNA and imaged the resulting capsids using negative-stain electron microscopy (data not shown). The in vivo-expanded capsids with DNA do not appear to be affected by heat treatment, other than the possible loss of DNA by a few capsids. Because the preparation of in vivo-expanded capsids lacking DNA necessarily results in a small population of procapsids, heat treatment of this sample cannot be definitive. However, the majority of the imaged capsids did not have released pentons. These results suggest the pentons are released during heat expansion.

Perhaps release of the pentons during heat expansion is not surprising, since during procapsid maturation, the radial position of the penton moves outward 75 Å from 610 Å to

685 Å (Zhang et al., 2000). In comparison, the average radial change incurred during expansion of the entire capsid is only 50 Å (Zhang et al., 2000). The penton undergoes the largest radial change of the seven quasiequivalent coat protein subunits within the P22 icosahedral lattice, accounting for the overall polyhedral appearance of the in vivo-expanded empty phage head (Figs. 2 *B* and 3 *B*).

Our observations do not indicate if heat expansion follows the same pathway as in vivo expansion other than that the resulting structure is the same but for the loss of pentons. If expansion occurs via a different mechanism with heat treatment, as opposed to in vivo DNA packaging, then the release of pentons could simply be a result of excess energy. However, the large movement the pentons undergo during in vivo expansion, combined with the high degree of similarities in the remaining heat-expanded versus in vivo-expanded capsid lattices, leads us to favor a heat expansion mechanism that is similar to that of in vivo expansion. As additional support for our notion that heat expansion follows a similar pathway as in vivo expansion, the in vitro expansion of the bacteriophage HK97 has been thoroughly characterized (Lata et al., 2000; Conway et al., 2001). In this case, expansion of HK97 was induced by low pH rather than heat, but was shown to be similar to the in vivo pathway.

Assuming heat expansion follows a similar pathway to in vivo expansion, we propose that release of the penton during heat expansion is the result of failure to stop the outward movement of the penton that normally occurs during in vivo expansion. Fig. 6 shows the conformation of a penton subunit with respect to its neighboring hexon subunit in both the empty phage head and the procapsid (Thuman-Commike et al., 1999). We denote the region of interaction between the hexon and penton subunits as the penton hinge. In the procapsid (Fig. 6 *B*), this hinge is partially closed forming a V shape, but in the in vivo-expanded empty phage head, this hinge is wide open and flat (Fig. 6 *C*). In the heat-expanded capsid, this hinge is broken and the penton subunit released (Fig. 6 *D*). We propose that capsid protein interactions at this hinge region become unstable during heat expansion and account for penton release (Fig. 6 *E*).

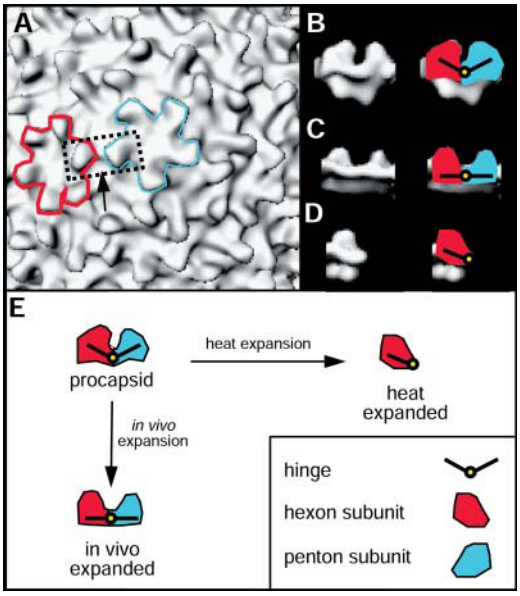

FIGURE 6 Depiction of penton hinge formed between neighboring penton and hexon subunits. (*A*) Surface representation of the in vivo-expanded empty phage head indicating the position of the penton hinge. Outlined in solid is a penton and hexon. The dotted box denotes the region of a single penton and hexon subunit that was computationally extracted for panels *B* and *C*, with the arrow indicating the viewing direction. (*B–D*) Side view of the penton hinge between a hexon and penton subunit in the bacteriophage P22 (*B*) procapsid, (*C*) in vivo-expanded empty phage head, and (*D*) heat-expanded capsid. For the procapsid, the penton hinge was computationally extracted from a previously determined scaffolding-containing P22 procapsid (Thuman-Commike et al., 1999). (*E*) Cartoon representation of the penton hinge transformation during both heat expansion and in vivo expansion. Notice that in the procapsid, the hinge is partially closed with the penton and hexon subunit tips near each another. After in vivo expansion, the hinge is open, resulting in a flat capsid floor and a greater distance between the penton and hexon subunits tips. After heat expansion, the hinge is broken and the penton subunit is released.

Possible mechanism for the stabilization of pentons during in vivo expansion

Why does the outward movement of the penton fail to stop during heat-induced expansion? The hexon subunits surrounding the penton hole in the heat-expanded capsid do not extend as far radially outward as those in the in vivo-expanded empty phage head (Fig. 4 *D*, *outlined region*). This could indicate that the heat-expanded hexons fail to undergo a conformational change required to maintain stability during expansion. Previous investigations have shown that expansion results in an increase in stability of capsids (Galisteo and King, 1993; Steven et al., 1992; Ross et al., 1985); therefore we find it unlikely, though possible, that the hexons would undergo the conformational transition usual to the maturation of the capsid and then collapse back to the less stable procapsid conformation. Instead, we prefer a model whereby accessory proteins, such as the pilot proteins, gp7, 16, and 20, that have been proposed to be located to the pentons (Thomas and Prevelige, 1991), interact with the DNA and the penton coat proteins keeping the pentons from releasing during DNA packaging. The pilot proteins are still within the in vivo-expanded heads, but are released from the heat-expanded heads (Casjens and King, 1974, Fig. 1 *a*). Thus, these accessory proteins could stabilize interactions at the hexon-penton interface during dsDNA packaging. The pilot proteins (10–20 copies each of the products of genes 7, 16, and 20) are required for phage viability but not for assembly of procapsids (Botstein et al., 1973; Casjens and King, 1974). Addition of gp16 increases the rate of in vitro procapsid assembly reactions using purified coat and scaffolding proteins (Thomas and Prevelige, 1991). Thomas and Prevelige (1991) also showed morphological differences between the capsids assembled with and without gp16. These differences

have not yet been investigated in detail, but they suggest that gp16 may play a role in the organization of the coat and scaffolding proteins during assembly. Indeed, gp16 interacts with both gp20 and coat proteins in vitro (Thomas and Prevelige, 1991).

In addition to the possible role of pilot proteins in stabilizing capsid structure, DNA is also likely to play a role. A previously proposed DNA insertion mechanism involves winding the DNA along the inner procapsid surface, filling the capsid from the outermost radius inward (Zhang et al., 2000). As DNA fills the capsid during in vivo expansion, the hexon subunits undergo a conformational change resulting in outward movement of the hexon-penton interface (Prasad et al., 1993; Zhang et al., 2000). Based on our results, we propose that in vivo the interactions of the DNA with capsid proteins and pilot proteins could stabilize the penton hinge, preventing penton release. In the heat-expanded capsid, however, the interactions with capsid proteins and pilot proteins are disrupted, perhaps causing release of the pilot proteins. Thus, in our model the interaction between the penton and hexon at the hinge would be stressed from the extra outward movement, forcing the penton to be released either due to steric hindrance or instability at the hinge.

It is unlikely that DNA would be directly interacting with coat protein at the penton positions because of the sharp bends required of the DNA to make contact with the pentons, but DNA might come into contact with the penton hinge region next to the hexons. Although interactions between any capsid proteins and the DNA in P22 have not been directly observed (Zhang et al., 2000), this may be due to the lack of icosahedral symmetry of the DNA within the capsid. Regardless, the close proximity of the DNA to the capsid shell and penton hinge, particularly during expansion, could serve to anchor the penton in place within the capsid, perhaps through interactions with the pilot proteins. Differential scanning calorimetry of P22 procapsids has shown that the expansion process is exothermic, producing an expanded capsid that is in a lower energy state than the procapsid (Galisteo and King, 1993). This suggests that after expansion has been completed, the DNA and/or pilot proteins are no longer required for penton stability, accounting for the continued presence of the pentons even after the DNA has been released from the capsid.

Penton release: a recurring theme in dsDNA viruses

Morphogenesis is a recurring theme in the assembly of dsDNA viruses. Adenoviruses, herpeseviruses, and dsDNA isometric bacteriophages such as lambda, HK97, and P22 undergo a capsid maturation process involving the transformation of an initial precursor capsid to a mature virion (D'Halluin et al., 1978; King and Chiu, 1997; Rixon, 1993; Casjens and Hendrix, 1988). The various conformational changes that occur during this transformation, including scaffolding exit, capsid lattice rearrangement, and capsid enlargement, demonstrate that these viral proteins possess an innate malleability during their life cycle and that many such transformations are similar among diverse groups of viruses.

Here we observe another large-scale conformational change—release of pentons during chemical or heat expansion—broadening this recurring theme of large-scale conformational changes. Penton release has been observed in other bacteriophage and mammalian viruses, in addition to P22 bacteriophage. In adenovirus (Prage et al., 1970) and herpesvirus (Newcomb et al., 1993), chemical treatments have been shown to release the pentons from their capsids. In these cases, interactions can be identified that play a role similar to what we propose above, whereby DNA and/or pilots interact with coat protein to prevent penton release. Specifically, for adenovirus, the interaction of hexon protein β-barrels with the penton protein are proposed to have a role in penton protein release during cell entry (Stewart et al., 1993). In the case of herpesvirus, it would seem likely that the triplex proteins, which are located between the pentons and hexons and are also released with herpesvirus pentons (Newcomb et al., 1993), perform this stabilization function. In bacteriophage T4 (Muller-Salamin et al., 1977) penton release also results from treatment with a denaturant. In the bacteriophage, penton release has no physiological role since DNA is transferred to the host cell through the portal complex. However, the fact that both mammalian viruses and bacteriophage show this loss of pentons indicates the universality of the instability of penton-hexon interactions.

The diverse conformational flexibility of the coat proteins within these various capsids contrasted with their similarities in morphogenesis is striking. The ability of the various capsids to release pentons suggests common interactions required for capsid stabilization beyond that previously observed.

We thank Carole Capen for preparation of samples, Dr. Barrie Greene for critical review of this manuscript, and Drs. Dennis Brown, Sandra Weller, and Peter Prevelige for helpful discussions.

This work was supported by National Institutes of Health grant GM53567 to C.M.T. A.M. is supported by grants from the W. M. Keck Foundation and the National Institutes of Health. Support for the electron cryomicroscopy facilities was obtained from the National Science Foundation, the W. M. Keck Foundation, the National Institutes of Health, the Markey Center for Structural Biology, and Purdue University.

REFERENCES

Bazinet, C., and J. King. 1985. The DNA translocating vertex of dsDNA bacteriophage. *Annu. Rev. Microbiol.* 39:109–129.

Botstein, D., C. H. Waddell, and J. King. 1973. Mechanism of head assembly and DNA encapsulation in Salmonella phage P22. I. Genes, proteins, structures and DNA maturation. *J. Mol. Biol.* 80:669–695.

Capen, C. M., and C. M. Teschke. 2000. Folding defects caused by single amino acid substitutions in a subunit are not alleviated by assembly. *Biochemistry*. 39:1142–1152.

Casjens, S., and R. Hendrix. 1988. Control mechanisms in dsDNA bacteriophage assembly. *In* The Bacteriophages. R. Calender, editor. Plenum Publishing, New York. 15–91.

Casjens, S., and J. King. 1974. P22 morphogenesis. I: Catalytic scaffolding protein in capsid assembly. *J. Supramol. Struct.* 2:202–224.

Cerritelli, M. E., N. Cheng, A. H. Rosenberg, C. E. McPherson, F. P. Booy, and A. C. Steven. 1997. Encapsidated conformation of bacteriophage T7 DNA. *Cell.* 91:271–280.

Conway, J. F., W. R. Wikoff, N. Cheng, R. L. Duda, R. W. Hendrix, J. E. Johnson, and A. C. Steven. 2001. Virus maturation involving large subunit rotations and local refolding. *Science.* 292:744–748.

D'Halluin, J.-C. M., G. R. Martin, G. Torpier, and P. Boulanger. 1978. Adenovirus type 2 assembly analysed by reversible cross-linking of labile intermediates. *J. Virol.* 26:357–363.

Earnshaw, W., S. Casjens, and S. C. Harrison. 1976. Assembly of the head of bacteriophage P22: X-ray diffraction from heads, proheads and related structures. *J. Mol. Biol.* 104:387–410.

Frank, J., A. Verschoor, and M. Boublik. 1981. Computer averaging of electron micrographs of 40S ribosomal subunits. *Science.* 214:1353–1355.

Fuller, M. T., and J. King. 1981. Purification of the coat and scaffolding protein from procapsids of bacteriophages P22. *Virology.* 112:529–547.

Galisteo, M. L., and J. King. 1993. Conformational transformations in the protein lattice of phage P22 procapsids. *Biophys. J.* 65:227–235.

King, J., D. Botstein, S. Casjens, W. Earnshaw, S. Harrison, and E. Lenk. 1976. Structure and assembly of the capsid of bacteriophage P22. *Philos. Trans. R. Soc. Lond. B Biol. Sci.* 276:37–49.

King, J., and S. Casjens. 1974. Catalytic head assembling protein in virus morphogenesis. *Nature.* 251:112–119.

King, J., and W. Chiu. 1997. The procapsid transition in double-stranded DNA bacteriophages. *In* Structural Biology of Viruses. W. Chiu, R. M. Burnett, and R. L. Garcea, editors. Oxford University Press, New York. 288–311.

King, J., C. Hall, and S. Casjens. 1978. Control of the synthesis of phage P22 scaffolding protein is coupled to capsid assembly. *Cell.* 15:551–560.

King, J., E. V. Lenk, and D. Botstein. 1973. Mechanism of head assembly and DNA maturation in salmonella phage P22. II. Morphogenetic pathway. *J. Mol. Biol.* 80:697–731.

Lata, R., J. F. Conway, N. Cheng, R. L. Duda, R. W. Hendrix, W. R. Wikoff, J. E. Johnson, H. Tsuruta, and A. C. Steven. 2000. Maturation dynamics of a viral capsid: visualization of transitional intermediate state, *Cell* 100:253–263.

Lepault, J., J. Dubochet, W. Baschong, and E. Kellenberger. 1987. Organization of double-stranded DNA in bacteriophages: a study by cryo-electron microscopy of vitrified samples. *EMBO J.* 6:1507–1512.

Marvik, O. J., T. Dokland, R. H. Nokling, E. Jacobsen, T. Larsen, and B. H. Lindqvist. 1995. The capsid size-determining protein Sid forms an external scaffold on phage P4 procapsids. *J. Mol. Biol.* 251:59–75.

Muller-Salamin, L., L. Onorato, and M. K. Showe. 1977. Localization of minor protein components of the head of bacteriophage T4. *J. Virol.* 24:121–134.

Newcomb, W. W., B. L. Trus, F. P. Booy, A. C. Steven, J. S. Wall, and J. C. Brown. 1993. Structure of the herpes simplex virus capsid: molecular composition of the pentons and the triplexes. *J. Mol. Biol.* 232: 499–511.

Parker, M. H., and P. E. J. Prevelige. 1998. Electrostatic interactions drive scaffolding/coat binding and procapsid maturation in bacteriophage P22. *Virology.* 250:337–349.

Prage, L., U. Pettersson, S. Hoglund, K. Lonberg-Holm, and L. Philipson. 1970. Structural proteins of adenoviruses. IV. Sequential degradation of the adenovirus type 2 virion. *Virology.* 42:341–358.

Prasad, B. V. V., P. E. Prevelige, E. Marietta, R. O. Chen, D. Thomas, J. King, and W. Chiu. 1993. Three-dimensional transformation of capsids associated with genome packaging in a bacterial virus. *J. Mol. Biol.* 231:65–74.

Prevelige, P. E., T. J. Dennis, and J. King. 1988. Scaffolding protein regulates the polymerization of P22 coat subunits into icosahedral shells in vitro. *J. Mol. Biol.* 202:743–757.

Radermacher, M. 1988. Three-dimensional reconstruction of single particles from random and nonrandom tilt series. *J. Electron Microsc. Tech.* 9:359–394.

Rixon, F. J. 1993. Structure and assembly of herpesviruses. *Semin. Virol.* 4:135–144.

Ross, P. D., L. W. Black, M. E. Bisher, and A. C. Steven. 1985. Assembly-dependent conformational changes in a viral capsid protein. Calorimetric comparison of successive conformational states of the gp23 surface lattice of bacteriophage T7. *J. Mol. Biol.* 183:353–364.

Serwer, P., S. Hayes, and G. Griess. 1986. Determination of a particle's radius by two-dimensional agarose gel electrophoresis. *Anal. Biochem.* 152:339–345.

Steven, A. C. 1993. Conformational change—an alternative source?: Exothermic phage transition inphage capsid maturation. *Biophys. J.* 65:5–6.

Steven, A. C., H. L. Greenstone, F. P. Booy, L. W. Black, and P. D. Ross. 1992. Conformational changes of a viral capsid protein. Thermodynamic rationale for proteolytic regulation of bacteriophage T4 capsid expansion, co-operativity, and super-stabilization by soc binding. *J. Mol. Biol.* 228:870–884.

Stewart, P. L., S. D. Fuller, and R. M. Burnett. 1993. Difference imaging of adenovirus: bridging the resolution gap between x-ray crystallography and electron microscopy. *EMBO J.* 12:2589–2599.

Teschke, C., and D. Fong. 1996. Interactions between coat and scaffolding proteins of phage P22 are altered in vitro by amino acid substitutions in coat protein that causes a cold-sensitive phenotype. *Biochemistry.* 35:14831–14840.

Teschke, C., and J. King. 1993. Folding of the phage P22 coat protein in vitro. *Biochemistry.* 32:10839–10847.

Thomas, D., and P. Prevelige. 1991. A pilot protein participates in the initiation of P22 procapsid assembly. *Virology.* 182:673–681.

Thuman-Commike, P., B. Greene, J. Malinski, M. Burbea, A. McGough, W. Chiu, and P. E. J. Prevelige. 1999. Mechanism of scaffolding-directed virus assembly suggested by comparison of scaffolding-containing and scaffolding-lacking P22 procapsids. *Biophys. J.* 76:3267–3277.

Tuma, R., P. E. J. Prevelige, and G. J. J. Thomas. 1998. Mechanism of capsid maturation in a double-stranded DNA virus. *Proc. Natl. Acad. Sci. USA.* 95:9885–9890.

van Heel, M. 1987. Similarity measures between images. *Ultramicroscopy.* 21:95–100.

Zhang, Z., B. Greene, P. Thuman-Commike, J. Jakana, P. Prevelige, J. King, and W. Chiu. 2000. Visualization of the maturation transition in bacteriophage P22 by electron cryomicroscopy. *J. Mol. Biol.* 297:615–626.